

Toward Personalized Federated Node Classification in One-shot Communication

Guochen Yan[†] Xunkai Li[‡] Luyuan Xie[#] Wentao Zhang^b
Qingni Shen[#] Yuejian Fang[#] Zhonghai Wu[#]

[†]School of Computer Science, Peking University

[‡]School of Computer Science, Beijing Institution of Technology

[#]School of Software and Microelectronics, Peking University

^bCenter for Machine Learning Research, Peking University

Guochen_Yan@outlook.com, cs.xunkai.li@gmail.com, 2201110745@stu.pku.edu.cn, wentao.zhang@pku.edu.cn,
qingnishen@ss.pku.edu.cn, fangyj@ss.pku.edu.cn, wuzh@pku.edu.cn

Abstract—Federated Graph Learning (FGL) has emerged as a promising paradigm for breaking data silos in distributed private graphs data management. In practical scenarios involving complex and heterogeneous distributed graph data, personalized Federated Graph Learning (pFGL) aims to enhance model utility by training personalized models tailored to individual client needs, rather than relying on a universal global model. However, existing pFGL methods often require numerous communication rounds under heterogeneous client graphs, leading to significant security concerns and communication overhead. While One-shot Federated Learning (OFL) addresses these issues by enabling collaboration in a single round, existing OFL methods are designed for image-based tasks and ineffective for graph data, leaving a critical gap in the field. Additionally, personalized models often suffer from bias, failing to generalize effectively to minority data. To address these challenges, we propose the first one-shot personalized federated graph learning method for node classification, compatible with the Secure Aggregation protocol for privacy preservation. Specifically, for effective graph learning in a single communication round, our method estimates and aggregates class-wise feature distribution statistics to construct a global pseudo-graph on the server, facilitating the training of a global graph model. Moreover, to mitigate bias, we introduce a two-stage personalized training approach that adaptively balances local personal information and global insights from the pseudo-graph, improving both personalization and generalization. Extensive experiments conducted on 8 multi-scale graph datasets demonstrate that our method significantly outperforms state-of-the-art baselines across various settings.

Index Terms—graph, one-shot federated learning, personalized federated graph learning

I. INTRODUCTION

Graphs are widely employed to model complex relationships between entities across a variety of domains, such as recommendation systems [1]–[3], finance [4]–[6], and biomedicine [7]–[9]. While various algorithms and models [10]–[13] have been proposed to analyze graph data effectively, most of them assume a centralized setting where graph data from different sources are aggregated together. However, collecting and managing such graph data is often costly, impractical, and presents significant privacy risks in many cases. For example, in healthcare applications, sharing patient relation graphs across institutions can expose sensitive medical and personal identity information [14]–[16]. Similarly,

in competing enterprises, graph data with potential commercial secrets are often strictly managed and stored in confidential databases [17], [18], making centralized data collection and management infeasible.

To address the tension between the need for vast datasets and the growing demand for privacy protection, Federated Graph Learning (FGL) has emerged as a viable solution. FGL enables collaborative model training across distributed graph data without the need for data centralization, preserving privacy and improving security. While FGL has shown its potential in collaborative training, it faces two significant limitations: 1) Typical FGL struggles with personalizing models for joint improvement effectively due to heterogeneous graph data across clients. This heterogeneity arises from differences in both node and structural properties, with adjacent nodes influencing each other, further complicating personalization. 2) It requires iterative communication between clients and the server, which would incur security concerns (e.g. man-in-the-middle attacks [19]–[22]) and efficiency concerns due to communication overhead between clients and the server [23]–[25]. These limitations can be mitigated by integrating personalized federated graph learning (pFGL) and one-shot federated learning (OFL), which offer novel solutions to improve communication efficiency and model personalization.

To address these challenges, we explore the integration of pFGL and OFL within the FGL paradigm. Methods of pFGL allow for personalized model training by focusing on individual client graph data. OFL reduces the communication overhead by enabling a single communication round, thereby circumventing security risks such as man-in-the-middle attacks and improve the communication efficiency [26], [27]. However, both existing pFGL and OFL methods face challenges in FGL. Specifically, they exhibit the following limitations:

L1: Ineffectiveness for graph learning in one communication round. Existing pFGL methods [28]–[30] rely on iterative communication for model optimization, making them ineffective within one communication round. Most methods also often fail to support heterogeneous models, as they primarily rely on aggregating model parameters. Meanwhile, existing OFL methods, which focus primarily on image-

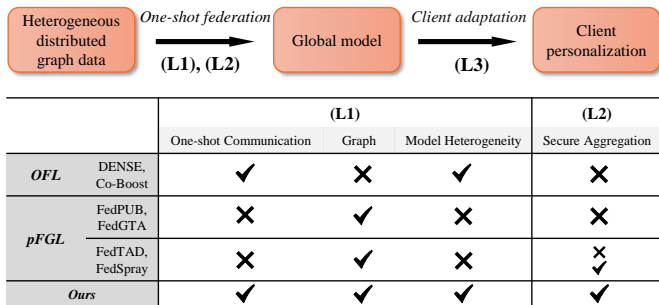


Fig. 1: The key limitations of existing methods. **L1**: Ineffectiveness for graph learning in one communication round. **L2**: Incompatibility with Secure Aggregation. **L3**: Imbalance between personalization and local generalization in personalization. The table details the limitations within **L1** and **L2**, and our method stands out as the only method capable of supporting one-shot federated learning for graph data while accommodating model heterogeneity and Secure Aggregation.

based tasks, are incompatible with graph data. The ensemble-based OFL methods [27], [31], [32] can invert images from ensemble models, but struggle with graph data due to the inter-dependencies between nodes. The distillation-based OFL also faces the problems of distilling inter-related graphs. The generative-based OFL methods [33]–[35] rely on pre-trained generative models (e.g. Stable Diffusion [36]), which are not suitable for graph generation.

L2: Incompatibility with Secure Aggregation. Secure Aggregation is a widely used protocol [37], [38] designed to safeguard client privacy during the federated aggregation process. However, most existing pFGL and OFL methods require the uploading of raw model parameters or side information (e.g. additional vectors in FedPUB and FedGTA) independently, which complicates the aggregation process (e.g. ensemble or cosine similarity calculation) and prevents the implementation of privacy-preserving weighted averages.

L3: Imbalance between personalization and local generalization in personalization. Local graph data often exhibit a significant imbalance in both quantity and topology, as illustrated in Fig. 2a. Personalized models tend to be biased toward major classes (with larger quantities and high homophily that form compact communities) while neglecting minor classes with fewer samples and often surrounded by nodes from major classes. This imbalance leads to a degradation in overall model performance, particularly in underrepresented classes. A detailed empirical analysis is provided in Fig.2b. The left panel shows that existing personalized methods result in models heavily biased toward majority classes (class 3 and class 5, with a total of 180 samples) while failing to adequately represent minority classes (class 1 and class 2, with only 64 samples), highlighting the limitations of current approaches in handling imbalanced graph data.

To overcome these limitations, we first propose a One-shot personalized Federated Graph Learning (O-pFGL) method. Our method supports model heterogeneity and integrates with

the Secure Aggregation protocol to ensure privacy. Specifically, for **L1** and **L2**, clients upload estimated feature distribution statistics instead of raw model parameters, and the server securely aggregates these statistics to generate a global pseudo-graph. This global pseudo-graph is subsequently utilized to train personalized models on clients, eliminating the need for direct model parameter exchanges and preventing model theft. This design streamlines the FGL process by reducing communication overhead and securely abstracting client-specific information into actionable insights in distributed and private graph data management. Furthermore, To address **L3** and improve the personalization-generalization balance, we introduce a two-stage personalized training approach. In the first stage, clients train a global model based on the pseudo-graph, which captures global knowledge and serves as both a fixed teacher model and an initialization for subsequent fine-tuning. In the second stage, clients fine-tune the global model using their local graph data employing a node-adaptive distillation mechanism. This mechanism leverages the global knowledge from the teacher model to counteract biases toward majority classes, ensuring effective learning for minority classes and achieving a robust balance between personalization and generalization.

Our method significantly outperforms state-of-the-art baselines through comprehensive experiments conducted on eight graph datasets across various settings, including different graph scales, partition strategies, learning paradigms, and evaluation metrics. These experimental results demonstrate the superiority of our method in achieving a one-shot personalized federated graph learning solution that balances privacy, efficiency, and personalization. To sum up, our contributions are listed as follows:

- **New Problem.** To the best of our knowledge, we first investigate the one-shot personalized federated graph learning problem under both graph data heterogeneity and model heterogeneity.
- **New Method.** We propose a novel method that aggregates client statistics rather than model parameters to generate a global pseudo-graph, which is then used for two-stage personalized model training with node-adaptive distillation. Our method is compatible with Secure Aggregation and protects the model’s intellectual property.
- **SOTA Performance.** We conduct comprehensive experiments on 8 multi-scale graph datasets. Our method significantly outperforms the state-of-the-art baselines on both accuracy and F1-macro evaluations in all settings.

II. RELATED WORKS

A. Federated Graph Learning

With the rapid development of federated learning methods, recent works introduce federated graph learning to collaboratively train graph models [39] in a privacy-preserving manner and apply it to many applications [40]–[44]. From the graph level, each client possesses multiple completely disjoint graphs (e.g. molecular graphs). Recent works [45], [46] mainly focus

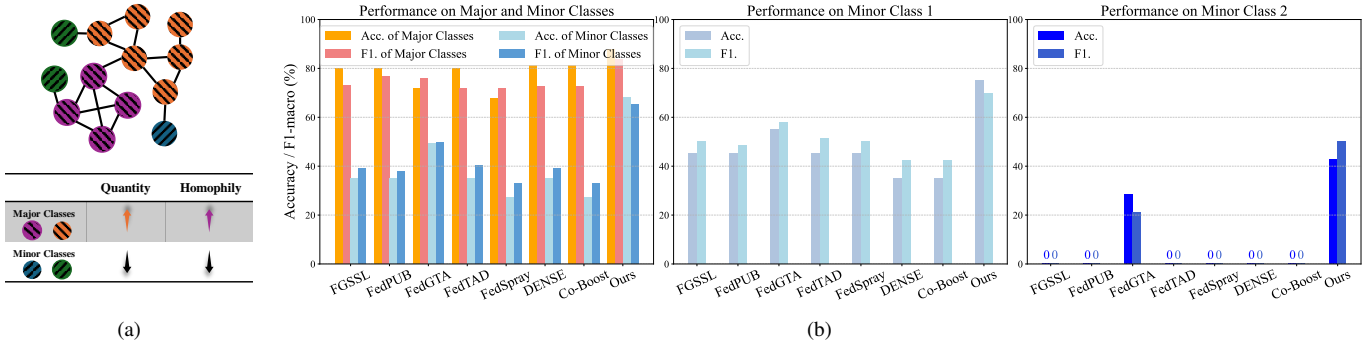


Fig. 2: (a) A toy example explains the major classes and minor classes. (b) The empirical analysis of a client on the CiteSeer dataset under the Louvain partition to illustrate **L3**. Left: Existing methods result in a biased model that neglects the minority. Middle: Existing methods’ and our’ performance in class 1 with 50 samples. Right: Existing methods’ and our’ performance in class 2 with 14 samples. The performance gap indicates a large margin and our method mitigates this gap largely.

on the intrinsic heterogeneity among graphs from different clients. From the sub-graph level, the graph possessed by each client can be regarded as a part of a larger global graph. To cope with heterogeneous graph data, GraphFL [47] adopts meta-learning for better generalization. FedGL [48] uploads the node embedding and prediction for global supervision but faces a heavy communication burden and potential privacy concerns. FGSSL [49] augments the local graph to mitigate the heterogeneity. To enhance the model utility on each client, personalized federated graph learning methods are proposed. FedPUB [28] generates random graphs to measure the similarity in model aggregation and conducts adaptive weight masks for better personalization. FedGTA [29] proposes topology-aware personalized optimization. AdaFGL [50] studies the structure non-IID problem. FedTAD [30] utilized ensemble local models to perform data-free distillation on the server. To complete missing connections between graphs of clients, FedSage [51] and FedDEP [52] additionally train a neighborhood generator. FedGCN [53] additionally uploads and downloads the encrypted neighbor features to supplement features of the neighborhood. For better representation of the minority in local graph data, FedSpray [54] learns local class-wise structure proxies to mitigate biased neighboring information. But it needs numerous communication rounds for optimization.

B. One-shot Federated Learning

One-shot federated learning largely reduces communication costs and circumvents potential man-in-the-middle attacks. Mainstream OFL methods can be categorized into 3 categories. (1) Ensemble-based: The original OFL study [26] ensembles local models and conducts knowledge distillation with public data. DENSE [27] utilizes the model inversion [55] to generate images from the ensemble model for distillation. FedOV [56] introduces the placeholders in the model prediction layer. IntactOFL [32] trains a MoE network by the generated images. Co-Boost [31] further optimizes the generated images and ensemble weights iteratively. (2) Distillation-based: DOSFL [57] and FedD3 [58] conduct dataset distillation locally and upload

distilled data for server-side training. (3) Generative-based: FedCAVE [33] trains VAEs for each client to generate similar images to mitigate the data heterogeneity. FedDISC [35] and FedDEO [34] utilize the pre-trained Stable Diffusion [36] to generate images to mitigate data heterogeneity. However, existing OFL methods mainly focus on image data. They are either incompatible or ineffective for graph learning.

III. PRELIMINARIES

A. Notations

Consider a federated graph learning setting with m clients, where each client possesses its local undirected graph. The k -th client possesses the graph $G_k(\mathcal{V}_k, \mathcal{E}_k)$ with $|\mathcal{E}_k|$ edges and $|\mathcal{V}_k| = N_k$ nodes. The corresponding node features matrix is denoted as $\mathbf{X}_k = \{\mathbf{x}_1, \dots, \mathbf{x}_{n_k}\} \in \mathbb{R}^{|\mathcal{V}_k| \times d}$, where d represents the dimension of node features and \mathbf{x}_i is the feature vector of node v_i . The adjacency matrix of the graph (including self-loops) is represented as $\hat{\mathbf{A}}_k \in \mathbb{R}^{|\mathcal{V}_k| \times |\mathcal{V}_k|}$. The labels of nodes in this local graph are denoted by $\mathbf{Y}_k = \{y_1, \dots, y_{n_k}\} \in \mathbb{R}^{|\mathcal{V}_k|}$.

In the semi-supervised node classification task, nodes on k -th client are partitioned into two subsets: labeled nodes $\mathcal{V}_{k,L}$ and unlabeled nodes $\mathcal{V}_{k,U}$. The corresponding labels are partitioned as $\mathbf{Y}_{k,L}$ and $\mathbf{Y}_{k,U}$, respectively. The neighborhood of node v_i in $G_k(\mathcal{V}_k, \mathcal{E}_k)$ is defined as $\mathcal{N}_{v_i} = \{u | \exists e_{u,v_i} \in \mathcal{E}_k\}$, where e_{u,v_i} is an edge connecting node u and v_i . Nodes across all clients’ local graphs are categorized into C distinct classes.

A Graph Neural Network (GNN) model [39] M takes the node feature matrix \mathbf{X} and the normalized adjacency matrix $\hat{\mathbf{A}}$ as input and outputs the logits $o \in \mathbb{R}^C$, which can be expressed as $o = M(\hat{\mathbf{A}}, \mathbf{X})$. For the prediction of a single node v_i , this is simplified to $o_i = M(\mathbf{x}_i)$. The cross-entropy loss is denoted by L_{ce} and the KL divergence loss is denoted by L_{kl} .

B. Problem Formulation

We formulate the problem of one-shot personalized federated graph learning for node classification as the following

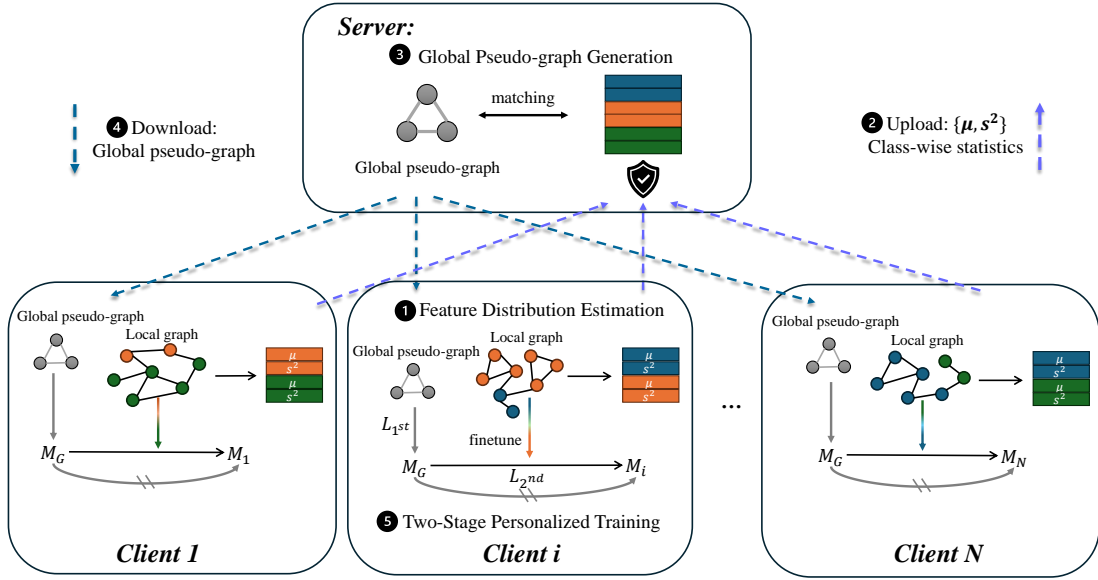


Fig. 3: The overall pipeline of our proposed method. μ and s^2 with different colors represent the class-wise sample mean and variance of propagated node features on each clients. M_G represents the model trained solely on the global pseudo-graph and M_i represents the personalized model. Our method consists of 5 steps: 1. Feature distribution estimation on the client-side, 2. Uploading class-wise feature distribution statistics to the server, 3. Global pseudo-graph generation on the server-side, 4. Server distributes the global pseudo-graph, 5. Two-stage personalized training on the client-side. The uploading and aggregation of clients' statistics could be protected by the Secure Aggregation protocol.

optimization objective:

$$\min \sum_{k=0}^{m-1} L(M_k, \mathbf{A}_k, \mathbf{X}_k, \mathbf{Y}_{k,U}), \quad (1)$$

where m represents the number of participating clients, each owning its local graph $G_k = (\mathcal{V}_k, \mathcal{E}_k)$. Each client trains its personalized model M_k . The objective in Eq. 1 aims to minimize the aggregated generalization loss L on their unlabeled node set across all clients within a single upload-download communication round.

C. Definitions

Definition 1: Node Degree. For a node $v_i \in \mathcal{V}$ in an undirected graph $G(\mathcal{V}, \mathcal{E})$, the node degree $d(v_i)$ is the number of the edges connected to v_i . Formally, $d(v_i) = |\{e_{v_i,u} | u \in \mathcal{V}\}|$.

Definition 2: Node Homophily. For a labeled node $v_i \in \mathcal{V}_L$ in an undirected graph $G(\mathcal{V}, \mathcal{E})$, The node homophily $h_{node}(v_i)$ quantifies the proportion of its labeled neighbors that share the same label y_{v_i} :

$$h_{node}(v_i) = \frac{|\{u | (u \in \mathcal{N}_{v_i} \cap \mathcal{V}_L) \text{ and } (y_{v_i} = y_u)\}|}{|\mathcal{N}_{v_i} \cap \mathcal{V}_L|}. \quad (2)$$

Definition 3: Accumulated Class Homophily. In an undirected graph $G(\mathcal{V}, \mathcal{E})$, The accumulated class homophily for class c is defined as:

$$H(c) = \sum_{u \in \mathcal{N}_c^G} h_{node}(u), \quad (3)$$

where $\mathcal{N}_c^G = \{v_i \in \mathcal{V}_L | y_i = c\}$ represents the set of nodes in G belonging to class c . Note that Accumulated class

homophily $H(c)$ considers both the number of nodes in class c and their topology. A higher $H(c)$ would indicate that nodes of class c are numerous and exhibit strong homophily, making them more predictable for a vanilla GNN model.

Definition 4: Class-aware Distillation Factor. Using Accumulated Class Homophily, we define the Class-aware Distillation Factor as:

$$w_{dist}(c) = \frac{1}{1 + \log(H(c) + 1)}. \quad (4)$$

Classes with lower $H(c)$ require more distillation from a balanced global model. These factors are organized into a vector $\mathbf{w}_{dist} \in \mathbb{R}^C$ where the i -th entry corresponds to $w_{dist}(i)$ for class i . This vector is used to determine the γ_i for each node, as described in Sec. IV-D.

IV. PROPOSED METHOD

A. Overall Pipeline

The overall proposed one-shot personalized federated graph learning method is illustrated in Fig. 3. It comprises five key steps. (1) Each client utilizes its local graph data to estimate the class-wise feature distribution and compute corresponding statistics; (2) Each client uploads its locally estimated class-wise statistics to the server; (3) The server aggregates the uploaded statistics using a weighted average to recover the global class-wise feature distribution. Based on the recovered distribution, the server generates a small-size global pseudo-graph (including adjacency matrix and node features); (4) The server distributes the generated global pseudo-graph to all clients; (5) Each client performs two-stage local personalized

model training using both local graph data and the downloaded global pseudo-graph, resulting in a model with improved personalization and generalization.

Specifically, in the first step, we propose a homophily-guided reliable node expansion strategy as an augmentation to enhance the precision of the distribution statistics. In the third step, we adapt techniques from graph condensation to facilitate the generation of the global pseudo-graph. In the fifth step, we address a critical issue that existing personalized methods neglect minor and blended nodes in imbalanced local graph data, which often leads to models biased toward the major nodes. We propose a two-stage personalized model training process with node-adaptive distillation, which helps achieve better personalization and generalization. The details are explained in the following sections.

B. Feature Distribution Estimation

To estimate the class-wise feature distribution locally, each client computes propagated node features using its local graph data. Specifically, on client k , the propagated features are calculated as:

$$\mathbf{X}_k^{prop} = \parallel_{i=0}^h \tilde{\mathbf{A}}^i \mathbf{X}_k, \quad (5)$$

where h is the propagation depth and \parallel represents the concatenation. Using the propagated features, we unbiasedly estimate the sample mean and sample variance of features for labeled nodes in each class:

$$\begin{aligned} \boldsymbol{\mu}_k^c &= \frac{1}{|\mathcal{V}_{k,L}^c|} \sum_{v_i \in \mathcal{V}_{k,L}^c} \mathbf{x}_i^{prop}, \\ \mathbf{s}_k^{2c} &= \frac{1}{|\mathcal{V}_{k,L}^c| - 1} \sum_{v_i \in \mathcal{V}_{k,L}^c} (\mathbf{x}_i^{prop} - \boldsymbol{\mu}_k^c)^2, \end{aligned} \quad (6)$$

where $\mathcal{V}_{k,L}^c$ denotes the labeled nodes of class c on client k . Note that statistics are computed only for classes with sufficient labeled nodes, determined by a client-specific threshold.

However, due to the limited number of labeled nodes, the above estimation may lack accuracy. To address this, we propose a Homophily-guided Reliable node Expansion (HRE) strategy as a plugin to further augment the estimation process on homophilic graphs. In HRE, we first apply Label Propagation to obtain the soft labels $\tilde{\mathbf{y}} \in \mathbb{R}^C$ for unlabeled nodes. We then identify reliable soft labels based on the following criteria:

- 1) Prediction Confidence: $\tilde{\mathbf{y}}_i(c') \geq f_{th}$. The soft label has high confidence.
- 2) Class Homophily: $c' \in \text{top}K(H)$. The predicted class c' has a high accumulated class homophily, making it likely that the node shares the same label with its neighbors.
- 3) Node Degree: $d(v_i) \geq d_{th}$. Nodes with higher degrees are prioritized, as more neighbors reduce the variance in predictions.

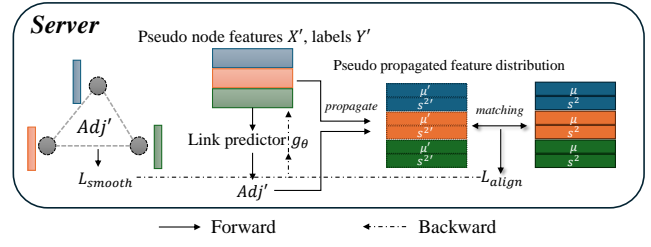


Fig. 4: The global pseudo-graph generation process on the server. $\boldsymbol{\mu}'$ and $\mathbf{s}^{2'}$ with different colors represent the class-wise sample mean and variance of the propagated node features in the global pseudo-graph, respectively.

Thus, the set of reliable nodes $\mathcal{V}_{k,r}$ with inferred true labels is defined as:

$$\begin{aligned} \mathcal{V}_{k,r} &= \{v_i | (v_i \in \mathcal{V}_{k,U}) \wedge (\tilde{\mathbf{y}}_i(c') \geq f_{th}) \wedge \\ &\quad (d(v_i) \geq d_{th}) \wedge (c' \in \text{top}K(H))\}, \\ c' &= \arg \max_{0 \leq i < C} \tilde{\mathbf{y}}(i), \end{aligned} \quad (7)$$

where $\text{top}K(H)$ is the set of classes with the highest K -values of accumulated class homophily $H(c)$, K , f_{th} and d_{th} are client-defined hyper-parameters. The reliable nodes $\mathcal{V}_{k,r}$ with their inferred labels expand the original labeled nodes set $\mathcal{V}_{k,L}$.

Using the expanded labeled nodes set, the estimation of feature distribution could be augmented as:

$$\begin{aligned} \boldsymbol{\mu}_k^c &= \frac{1}{|\mathcal{V}_{k,L}^c \cup \mathcal{V}_{k,r}^c|} \sum_{v_i \in \mathcal{V}_{k,L}^c \cup \mathcal{V}_{k,r}^c} \mathbf{x}_i^{prop}, \\ \mathbf{s}_k^{2c} &= \frac{1}{|\mathcal{V}_{k,L}^c \cup \mathcal{V}_{k,r}^c| - 1} \sum_{v_i \in \mathcal{V}_{k,L}^c \cup \mathcal{V}_{k,r}^c} (\mathbf{x}_i^{prop} - \boldsymbol{\mu}_k^c)^2, \end{aligned} \quad (8)$$

where $\mathcal{V}_{k,r}^c$ represents the subset of reliable nodes in $\mathcal{V}_{k,r}$ belonging to class c . This augmented process ensures a more accurate and robust estimation of class-wise feature distributions by incorporating reliable nodes into the computation.

C. Global Pseudo-Graph Generation

After clients estimate the class-wise feature distribution statistics $\{\boldsymbol{\mu}_k^c, \mathbf{s}_k^{2c}\}$, they upload them along with sample quantity of each class $\{N_k^c\}$ into the server. The server aggregates them to recover the global class-wise feature distribution. Specifically, the global mean and global variance of class c are computed unbiasedly as:

$$\begin{aligned} N^c &= \sum_k^m N_k^c, \\ \boldsymbol{\mu}^c &= \frac{1}{N^c} \sum_k^m N_k^c \boldsymbol{\mu}_k^c, \\ \mathbf{s}^{2c} &= \frac{1}{N^c - m} \left(\sum_k^m (N_k^c - 1) \mathbf{s}_k^{2c} + \sum_k^m N_k^c (\boldsymbol{\mu}_k^c - \boldsymbol{\mu}^c)^2 \right). \end{aligned} \quad (9)$$

Using the aggregated statistics, the server reconstructs the global distribution for each class, which is then used to guide the generation of a global pseudo-graph.

Inspired by techniques from the graph condensation [59]–[62], we generate a small-size global pseudo-graph $G' = \{\mathbf{A}', \mathbf{X}', \mathbf{Y}'\}$ by aligning its feature distribution with the aggregated global distribution. This pseudo-graph serves as a representative of the overall graph data across all clients. The generation process is illustrated in Fig. 4. To initialize G' , we first pre-set the node labels \mathbf{Y}' in the global pseudo-graph that the number of nodes for class c in the pseudo-graph set to $\max\{1, pN^c\}$, where p is a small fraction. The node features \mathbf{X}' are initialized from Gaussian noise and treated as trainable parameters. The adjacency matrix \mathbf{A}' is defined using a trainable link predictor g_θ . The connectivity between node i and j is given by:

$$\begin{aligned} \mathbf{A}'_{i,j} &= g_\theta(\mathbf{X}', \delta), \\ &= \mathbb{I}(\delta \leq \sigma(\frac{g_\theta(\mathbf{x}_i \| \mathbf{x}_j) + g_\theta(\mathbf{x}_j \| \mathbf{x}_i)}{2})), \end{aligned} \quad (10)$$

where σ denote the Sigmoid function, δ is a hyper-parameter to control sparsity, and $\|$ represents concatenation.

Following [62], to optimize the \mathbf{X}' and g_θ , we first propagate the node feature with \mathbf{A}' following the Eq. 5. Then we calculate the class-wise sample mean $\boldsymbol{\mu}'^c$ and sample variance \mathbf{s}'^{2c} of the propagated node features \mathbf{X}'^{prop} in the pseudo-graph following Eq. 6. Then we calculate the alignment loss:

$$L_{align} = \sum_{c=0}^{C-1} \lambda_c ((\boldsymbol{\mu}'^c - \boldsymbol{\mu}^c)^2 + (\mathbf{s}'^{2c} - \mathbf{s}^{2c})^2), \quad (11)$$

where λ_c represents the proportion of nodes belonging to class c relative to the total number of nodes. To ensure the smoothness of the pseudo-graph, smoothness loss is applied:

$$L_{smooth} = \frac{1}{\sum_{i,j} \mathbf{A}'_{i,j}} \sum_{i,j} \mathbf{A}'_{i,j} \exp(-\frac{\|\mathbf{x}_i - \mathbf{x}_j\|^2}{2}). \quad (12)$$

We could optimize the \mathbf{X}' and g_θ to generate the global pseudo-graph by the overall optimization objective:

$$\min_{\mathbf{X}', \theta} (L_{align} + \alpha L_{smooth}). \quad (13)$$

Once the global pseudo-graph is generated, it serves as an informative and compact representation of the overall graph data from all clients. The server distributes the global pseudo-graph to clients for further personalized training.

Privacy-preservation with Secure Aggregation. To further enhance security and privacy during the uploading and aggregation of $\{\boldsymbol{\mu}_k^c, \mathbf{s}_k^{2c}, N_k^c\}$, we demonstrate compatibility with the Secure Aggregation protocol. Secure Aggregation enables the server to compute the sum of large, user-held data vectors securely, without accessing individual client contributions. This property aligns well with the aggregation process in Eq. 9, as it can be expressed as a series of weighted average operations. The calculation of N^c and $\boldsymbol{\mu}^c$ are inherently weighted averages. Specifically:

$$N^c = \sum_k N_k^c, \quad \boldsymbol{\mu}^c = \frac{1}{N^c} \sum_k N_k^c \boldsymbol{\mu}_k^c, \quad (14)$$

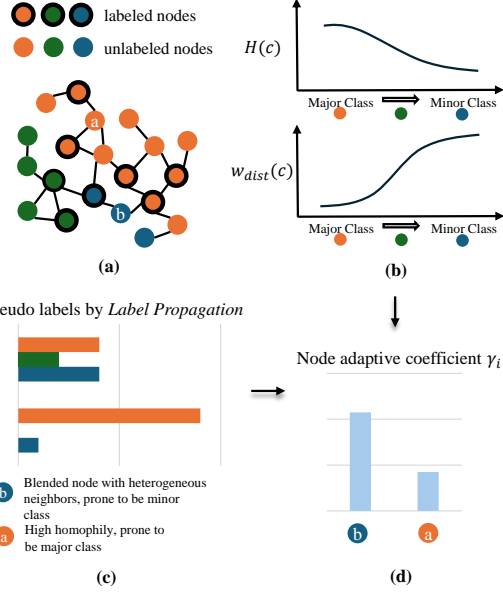


Fig. 5: The process to determine γ_i for each node in node adaptive distillation in the second stage. Node a is likely to belong to the **major class**, resulting in a relatively smaller γ_i , as calculated by the weighted average of w_{dist} . In contrast, the pseudo label of node b is mixed, with a considerable probability of being classified into the **minor class**, leading to a relatively larger γ_i .

The calculation of \mathbf{s}^{2c} , while more complex, can also be decomposed into weighted average operations. Decomposing the calculation of \mathbf{s}^{2c} in Eq. 9, we have:

$$\begin{aligned} \mathbf{s}^{2c} &= \frac{1}{N^c - m} \left(\sum_k (N_k^c - 1) \mathbf{s}_k^{2c} + \sum_k N_k^c (\boldsymbol{\mu}_k^c - \boldsymbol{\mu}^c)^2 \right), \\ &= \frac{\sum_k (N_k^c - 1) \mathbf{s}_k^{2c}}{N^c - m} \\ &\quad + \frac{\sum_k N_k^c (\boldsymbol{\mu}_k^c)^2 - 2\boldsymbol{\mu}^c \sum_k N_k^c \boldsymbol{\mu}_k^c + N^c \sum_k (\boldsymbol{\mu}_k^c)^2}{N^c - m}, \end{aligned} \quad (15)$$

Breaking this down further, the calculation involves the weighted averages of $(N_k^c - 1) \mathbf{s}_k^{2c}$, $N_k^c (\boldsymbol{\mu}_k^c)^2$ and $\boldsymbol{\mu}_k^c$. Thus, the entire aggregation process for $\{\boldsymbol{\mu}_k^c, \mathbf{s}_k^{2c}, N_k^c\}$ can be conducted without revealing individual client data contributions, making it fully compatible with Secure Aggregation.

D. Personalized Training with Node Adaptive Distillation

With the downloaded global pseudo-graph, each client trains its personalized model locally. Existing pFGL methods primarily focus on accuracy improvement. However, the imbalanced local graph data often results in biased models that perform well on major classes but neglect minority classes, as reflected by low F1-macro value. To achieve better personalization (high accuracy) and generalization (high F1-macro), we propose a two-stage adaptive personalized model training approach. The key idea is to leverage both the global information

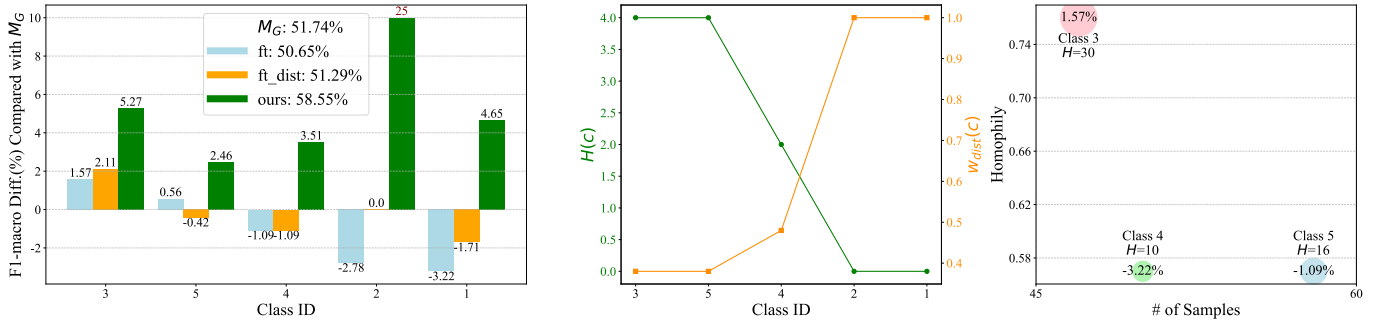


Fig. 6: An analysis of a client on the CiteSeer dataset. Left: The performance difference of our method (ours) and two variants (ft and ft_dist) compared with M_G trained solely on the global pseudo-graph. The ft and ft_dist methods exhibit overall degradation on F1-macro, while ours consistently achieves improvements across all classes. Middle: the value of H and w_{dist} of each class. The trend of H across classes aligns with the performance differences observed after fine-tuning (“ft”). Right: The value of H is influenced by both the number of samples and their homophily. Although class 4 has more samples, most of them have relatively low homophily, resulting in a smaller H value compared to class 3. The performance improvement after fine-tuning (ft) for class 4 is -1.09% while for class 3 it is +1.57%.

encapsulated in the global pseudo-graph and the local data, using a node-adaptive distillation strategy.

a) *Stage 1*: In the first stage, each client trains a local model M_G using only the global pseudo-graph, ensuring M_G to capture global, balanced knowledge and avoid bias from the local data:

$$L_{1st} = L_{ce}(M_G(\mathbf{A}', \mathbf{X}'), \mathbf{Y}'), \quad (16)$$

A copy of the resulting M_G is detached as a fixed teacher model for the next stage.

b) *Stage 2*: In the second stage, client k fine-tunes the M_G with local graph data to derive a personalized model M_i . However, fine-tuning on imbalanced local graph data often leads to over-fitting on major classes while forgetting minor class knowledge. As illustrated in Fig. 6, the fine-tuned model shows performance gain in major classes (class 3 and class 5) but suffers performance drop in minor classes (class 4, class 2, and class 1). Thus, the fine-tuned model suffers limited overall accuracy improvement and low F1-macro value.

To mitigate this, we propose to take advantage of the global knowledge of M_G and local personalized knowledge in local graph data to train a better M_i with the node adaptive distillation. For nodes of major classes, the model directly learns through supervised fine-tuning. For nodes of minor classes, M_i additionally leverages the predictive ability of M_G . The training objective for the second stage is:

$$L_{2nd} = L_{ft} + L_{dist}, \quad (17)$$

where L_{ft} is the cross-entropy loss for supervised fine-tuning on local data, and L_{dist} is a weighted sum of point-wise KL-divergence loss that distills global knowledge from M_G :

$$L_{dist} = \sum_{\mathbf{x}_i \in \mathbf{X}_k} \gamma_i L_{kl}(M_i(\mathbf{x}_i), M_G(\mathbf{x}_i)), \quad (18)$$

Here, γ_i is a node-specific weighting factor that controls the balance between local fine-tuning and global knowledge distillation. To determine the value of γ_i for each node, we

utilize the soft labels $\tilde{\mathbf{y}}_i$ obtained by Label Propagation in Sec. IV-B and \mathbf{w}_{dist} in Eq. 4:

$$\gamma_i = \beta \tilde{\mathbf{y}}_i \cdot \mathbf{w}_{dist}. \quad (19)$$

where β is a scaling hyper-parameter.

Intuitively explained, (1) if a node is predicted to class c with a small $w_{dist}(c)$ (e.g. node a in Fig. 5), it is likely to belong to a major class with high homophily. In this case, γ_i is small and model M_i primarily learns through supervised fine-tuning; (2) if a node is predicted to class c with a large $w_{dist}(c)$ or has a blended prediction across classes (e.g. node b in Fig. 5), it likely belongs to a minor class or has low homophily. These nodes are prone to being neglected during supervised fine-tuning. Thus γ_i should be large to incorporate corresponding global knowledge from M_G .

V. EXPERIMENTS

In this section, we provide comprehensive experiments to validate the effectiveness of our methods. We first describe the experimental setup including graph datasets with various scales and training settings, baselines including pFGL and OFL methods, metrics for evaluation, and hyper-parameter configurations. Our experiments are designed to address the following key research questions: **Q1**: Compared with other state-of-the-art methods, can our method achieve advantageous performance under different partitions? **Q2**: On large-scale graphs and the increasing number of clients, can our method remain its performance advantageous? **Q3**: What are the primary contributors to the observed performance improvements? **Q4**: Can our method achieve superior performance under both data and model heterogeneity? **Q5**: Can our method sustain its advantages in inductive learning scenarios? **Q6**: How efficient is the communication of our method?

A. Experimental Setup

a) *Datasets*: We conduct our experiments on 8 datasets considering both transductive and inductive learning settings.

TABLE I: Performance on three small-scale datasets under Louvain partition. Acc. represents accuracy(%) and F1 represents the F1-macro(%). # 1 indicates that the average performance ranks first among all methods.

Louvain	Cora				CiteSeer				PubMed				Avg. Acc.	Avg. F1
	10 Clients		20 Clients		10 Clients		20 Clients		10 Clients		20 Clients			
	Acc.	F1	Acc.	F1	Acc.	F1	Acc.	F1	Acc.	F1	Acc.	F1		
Standalone	67.17 ±0.38	41.79 ±0.52	61.57 ±0.84	30.35 ±0.59	59.82 ±0.12	42.70 ±0.34	57.86 ±0.62	36.44 ±0.52	81.74 ±0.06	64.61 ±0.18	81.84 ±0.04	57.95 ±0.62	68.33 # 8	45.64 # 3
FedAvg	69.68 ±0.48	45.10 ±0.75	63.21 ±0.45	31.77 ±0.64	63.92 ±0.10	45.97 ±0.43	61.51 ±0.27	40.60 ±0.40	78.24 ±0.08	42.24 ±0.13	78.59 ±0.14	41.60 ±0.28	69.19 # 7	41.21 # 8
FedPUB	68.50 ±0.38	43.35 ±0.27	62.52 ±0.27	30.96 ±0.25	61.80 ±0.37	43.96 ±1.05	59.40 ±0.29	37.59 ±0.19	81.63 ±0.54	63.39 ±0.69	81.41 ±0.14	56.81 ±1.94	69.21 # 6	46.01 # 2
FGSSL	70.04 ±0.19	45.74 ±0.49	63.20 ±0.36	31.89 ±0.40	64.17 ±0.33	46.14 ±0.24	62.11 ±0.69	41.14 ±0.82	78.23 ±0.03	41.99 ±0.22	78.41 ±0.22	41.21 ±0.35	69.36 # 3	41.35 # 5
FedGTA	42.61 ±0.76	23.47 ±1.06	37.03 ±1.34	14.74 ±0.76	67.12 ±1.58	52.68 ±1.81	62.02 ±0.83	42.78 ±0.92	75.99 ±1.21	57.48 ±1.44	64.01 ±0.98	36.47 ±1.33	58.13 # 10	37.94 # 10
FedTAD	70.10 ±0.22	45.57 ±0.27	63.16 ±0.44	31.72 ±0.52	63.93 ±0.27	44.59 ±0.41	62.32 ±0.46	41.04 ±0.55	78.21 ±0.31	42.45 ±0.80	78.64 ±0.11	41.66 ±0.16	69.39 # 2	41.17 # 9
FedSpray	63.14 ±1.73	40.82 ±1.54	60.15 ±1.05	29.30 ±0.61	54.89 ±4.24	39.56 ±3.58	55.43 ±0.79	36.77 ±0.63	77.89 ±1.67	64.23 ±2.03	80.28 ±0.30	49.29 ±0.73	65.30 # 9	43.33 # 4
DENSE	69.89 ±0.30	45.35 ±0.55	63.24 ±0.32	31.74 ±0.44	64.09 ±0.48	46.00 ±0.39	61.71 ±0.21	40.69 ±0.44	78.16 ±0.06	41.96 ±0.33	78.59 ±0.15	41.63 ±0.31	69.28 # 5	41.23 # 7
Co-Boost	69.95 ±0.40	45.43 ±0.52	63.21 ±0.41	31.70 ±0.49	64.21 ±0.27	46.00 ±0.11	61.89 ±0.42	40.83 ±0.54	78.13 ±0.05	41.84 ±0.22	78.67 ±0.10	41.76 ±0.27	69.34 # 4	41.26 # 6
Ours	76.43 ±1.24	61.58 ±2.16	69.84 ±1.76	49.37 ±1.98	71.61 ±0.40	58.24 ±0.96	68.69 ±0.04	50.26 ±0.80	82.71 ±0.03	66.40 ±0.34	82.04 ±0.20	58.79 ±0.68	75.22 # 1	57.44 # 1

TABLE II: The statistics of the datasets.

Dataset	Task	#Nodes	#Edges	#Classes	#Train/Val/Test
Cora	Transductive	2,708	10,556	7	20%/40%/40%
Citeseer	Transductive	3,327	4,732	6	20%/40%/40%
PubMed	Transductive	19,717	44,338	3	20%/40%/40%
Ogbn-arxiv	Transductive	169,343	1,166,243	40	60%/20%/20%
Ogbn-products	Transductive	2,449,029	61,859,140	47	10%/5%/85%
Flickr	Inductive	89,250	899,756	7	60%/20%/20%
Reddit	Inductive	232,965	114,615,892	41	80%/10%/10%
Reddit2	Inductive	232,965	23,213,838	41	65%/10%/25%

For the transductive setting, we use three small-scale graph datasets: Cora, CiteSeer, and PubMed from [63] and two large-scale OGB graph datasets [64]: ogbn-arxiv and ogbn-products. For the inductive setting, we use one medium-scale graph dataset: Flickr [65], and two large-scale graph datasets: Reddit [66] and Reddit2 [65]. A summary of these graph datasets is provided in Table II.

To simulate the distributed graphs in federated graph learning, we vary the number of clients and employ two advanced graph partitions: Louvain-based Label Imbalance Split and Metis-based Label Imbalance Split [67]. For small- and medium-scale datasets, we simulate 10 and 20 clients, while for large-scale datasets, we simulate 10, 20, and 40 clients.

b) Baselines: We compare our method with 9 baseline methods including 5 state-of-the-art FGL and pFGL methods¹: 1) FedGTA [29], 2) FedPUB [28], 3) FGSSL [49], 4) FedTAD [30], 5) FedSpray [54], which pays attention in personalization, and 2 state-of-the-art OFL methods: 6) DENSE [27], 7) Co-Boost [31]. We also include 8) Standalone,

¹We do not include FedSage [51] and AdaFGL [50]. FedSage needs additional communication rounds to train neighborhood generators. AdaFGL consists of two-stage federated optimization. They both need additional communication for federated optimization and cannot train models within one-shot communication.

which locally trains models without communication, and 9) FedAvg with fine-tuning, as additional comparison baselines.

In DENSE and Co-Boost, the generators are trained to generate node features, and the topology structure is constructed using the K -Nearest Neighbors strategy as outlined in [30]. Note that we perform an additional 3 to 100 rounds of fine-tuning on FGSSL, FedTAD, DENSE, and Co-Boost to ensure better personalized performance.

c) Metrics: To comprehensively evaluate the performance, we employ both accuracy and F1-macro metrics. F1-macro calculates the average F1 score across all classes, providing a more robust measure of the model’s generalization ability, particularly under imbalanced data conditions. For each experiment, we report the mean and standard deviation of accuracy(%) and F1-macro(%) across three runs.

d) Hyper-parameters: In our one-shot personalized federated graph learning setup, we limit the communication round to a single round. For each client, we employ a two-layer GCN [39] with the hidden layer dimension set to 64 by default. The number of local training epochs is tuned from 3 to 100. For baseline methods, hyper-parameters are set as recommended in their respective papers or fine-tuned for optimal overall performance. In our method, we keep the size of the generated global pseudo-graph as small as possible. On small-scale graph datasets, we set the number of nodes in each class in the global pseudo-graph as 1. We set p as 0.25%, 0.04%, 1%, 0.05%, 0.05% on ogbn-arxiv, ogbn-products, Flickr, Reddit, and Reddit2 datasets. We set f_{th} as 0.95 and tune d_{th} according to the scale of the graphs. We tune the β within [0.1, 1] to control the range of γ_i . For other hyper-parameters in global pseudo-graph generation, we adopt the setting in [62]. Under model heterogeneity, we adopt 10 different GNN models categorized into two types: coupled GNNs and decoupled GNNs. For coupled GNNs, we adopt

TABLE III: Performance on three small-scale datasets under Metis partition.

Metis	Cora				CiteSeer				PubMed				Avg. Acc.	Avg. F1
	10 Clients		20 Clients		10 Clients		20 Clients		10 Clients		20 Clients			
	Acc.	F1	Acc.	F1	Acc.	F1	Acc.	F1	Acc.	F1	Acc.	F1		
Standalone	75.15	31.00	71.57	20.89	64.72	37.36	61.36	26.19	83.24	56.61	83.24	55.21	73.21	37.88
	± 0.08	± 0.09	± 0.29	± 0.06	± 0.37	± 0.38	± 0.27	± 0.40	± 0.09	± 0.77	± 0.05	± 0.35	# 2	# 2
FedAvg	76.18	31.42	73.14	18.38	66.51	35.89	62.62	28.48	79.26	33.75	79.86	34.81	72.93	30.46
	± 0.14	± 0.08	± 0.22	± 0.39	± 0.34	± 0.54	± 0.48	± 0.38	± 0.09	± 0.18	± 0.09	± 0.05	# 5	# 7
FedPUB	75.31	32.00	72.32	20.16	64.94	37.50	60.73	29.40	82.69	56.44	82.98	50.51	73.16	37.67
	± 0.20	± 0.53	± 0.32	± 0.82	± 0.42	± 0.57	± 0.14	± 0.16	± 0.10	± 1.21	± 0.21	± 0.26	# 3	# 3
FGSSL	76.39	31.52	73.40	18.46	66.76	36.16	62.47	28.21	79.32	33.88	79.81	34.68	73.02	30.48
	± 0.15	± 0.25	± 0.34	± 0.41	± 0.06	± 0.16	± 0.32	± 0.53	± 0.09	± 0.12	± 0.16	± 0.22	# 4	# 6
FedGTA	53.85	11.74	55.04	10.60	64.03	31.33	59.43	20.04	78.57	46.47	74.34	35.18	64.21	25.89
	± 0.29	± 0.66	± 0.14	± 0.07	± 0.28	± 0.54	± 0.40	± 0.82	± 0.58	± 0.94	± 0.36	± 0.61	# 10	# 10
FedTAD	76.36	31.99	73.55	18.78	66.76	36.06	62.60	28.44	79.41	34.19	77.42	31.17	72.68	30.11
	± 0.26	± 0.22	± 0.37	± 0.31	± 0.26	± 0.42	± 0.40	± 0.20	± 0.07	± 0.13	± 0.47	± 0.52	# 6	# 8
FedSpray	74.31	31.95	71.44	21.49	62.49	36.04	58.98	29.35	81.02	60.97	81.05	40.51	71.55	36.72
	± 0.34	± 0.69	± 0.04	± 0.15	± 0.85	± 0.54	± 1.87	± 1.52	± 0.56	± 1.27	± 0.33	± 0.56	# 9	# 4
DENSE	76.21	31.64	72.62	20.19	65.62	37.88	61.36	29.66	79.29	33.81	79.94	34.87	72.51	31.34
	± 0.08	± 0.24	± 0.17	± 0.13	± 0.27	± 0.24	± 0.19	± 0.20	± 0.05	± 0.09	± 0.04	± 0.07	# 7	# 5
Co-Boost	76.54	31.90	73.42	18.45	64.55	31.37	61.30	25.87	76.56	29.89	79.98	35.04	72.06	28.75
	± 0.31	± 0.36	± 0.06	± 0.24	± 0.73	± 0.75	± 0.56	± 0.78	± 0.36	± 0.34	± 0.06	± 0.27	# 8	# 9
Ours	81.79	50.85	78.31	37.21	72.76	50.94	68.88	41.95	83.99	61.03	83.94	56.61	78.28	49.76
	± 0.23	± 1.27	± 0.88	± 1.96	± 0.24	± 0.80	± 0.22	± 0.25	± 0.18	± 1.21	± 0.05	± 1.36	# 1	# 1

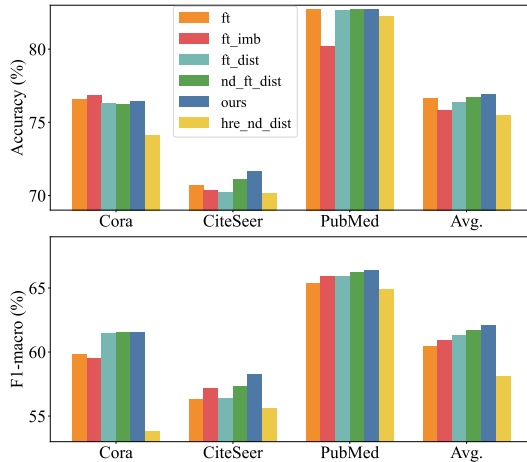


Fig. 7: Ablation study under Louvain partition.

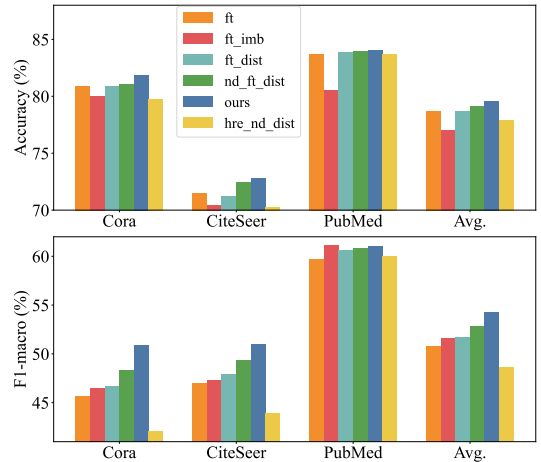


Fig. 8: Ablation study under Metis partition.

6 models which are: 2-layer GCN with 64, 128, 256, and 512 hidden dimension, 3-layer GCN with 64 and 512 hidden dimension. For decoupled GNNs, we adopt APPNP [10], SSGC [68], SGC ($K=2$) and SGC ($K=4$) [69].

e) Experimental Environments: The experimental machine is with Intel(R) Xeon(R) CPU E5-2680 v4@2.40GHz, and 6×NVIDIA GeForce RTX 3090. The operating system is Ubuntu 20.04 and the version of PyTorch is 2.1.2.

B. Experimental Results

1) Performance Comparison: To answer **Q1**, we conduct experiments and report the accuracy and F1-macro metrics. Table I and Table III present the results on three small-scale graph datasets under Louvain and Metis partitions, respectively. We make the following 5 observations. **(O1)** Our method consistently outperforms others, achieving at least

a +5.07% improvement in accuracy and +11.43% in F1-macro. **(O2)** Under the Louvain partition, the OFL and pFGL baselines (excluding FedGTA) outperform Standalone and FedAvg with fine-tuning, but the improvements are marginal ($\approx +1\%$). FedPUB shows a small F1-macro improvement (+0.37%), while other baselines show degradation compared to Standalone. **(O3)** FGSSL, FedTAD, DENSE, and Co-boost suffer a performance drop in F1-macro ($\approx -4\%$), indicating they may sacrifice predictive ability for minor classes during personalized fine-tuning. **(O4)** Under the more imbalanced Metis partition, all baselines fail to outperform Standalone, highlighting the ineffectiveness of current pFGL methods in handling extreme non-IID data in a single communication round. The state-of-the-art OFL methods (DENSE and Co-Boost) also have difficulty generating high-quality pseudo-data by the ensemble model when each model is trained on extreme

TABLE IV: Performance of methods on 10 clients with heterogeneous models under Louvain partition.

Louvain	Cora		CiteSeer		ogbn-arxiv		Avg. Acc.	Avg. F1
	Acc.	F1	Acc.	F1	Acc.	F1		
Standalone	68.37	43.51	62.50	43.94	66.13	19.60	65.67	35.68
	± 0.19	± 0.31	± 0.15	± 0.09	± 0.08	± 0.38	# 5	# 5
FedTAD	68.18	42.91	61.81	43.78	69.08	29.29	66.36	38.66
	± 0.22	± 0.34	± 0.18	± 0.14	± 0.08	± 0.44	# 4	# 4
FedSpray	65.73	42.23	53.14	39.13	68.63	22.25	62.50	34.54
	± 1.05	± 0.34	± 1.19	± 1.17	± 0.03	± 0.26	# 6	# 6
DENSE	68.15	43.02	62.31	44.27	69.03	29.64	66.50	38.98
	± 0.47	± 0.36	± 0.51	± 0.44	± 0.02	± 0.14	# 3	# 3
Co-Boost	68.38	43.13	62.22	44.23	69.08	29.88	66.56	39.08
	± 0.40	± 0.52	± 0.18	± 0.05	± 0.13	± 0.27	# 2	# 2
Ours	75.04	57.26	70.87	56.67	70.98	36.41	72.30	50.11
	± 0.50	± 1.93	± 0.21	± 0.20	± 0.09	± 0.43	# 1	# 1

TABLE V: Performance of methods on 10 clients with heterogeneous models under Metis partition.

Metis	Cora		CiteSeer		ogbn-arxiv		Avg. Acc.	Avg. F1
	Acc.	F1	Acc.	F1	Acc.	F1		
Standalone	74.33	30.73	64.53	37.52	65.18	25.25	68.01	31.17
	± 0.14	± 0.18	± 0.34	± 0.33	± 0.11	± 0.14	# 5	# 5
FedTAD	74.37	31.27	64.75	37.29	68.57	34.32	69.23	34.29
	± 0.30	± 0.25	± 0.64	± 0.34	± 0.08	± 0.44	# 2	# 2
FedSpray	73.09	30.84	60.38	34.96	67.39	27.88	66.95	31.23
	± 0.69	± 0.65	± 0.67	± 0.16	± 0.11	± 0.24	# 6	# 6
DENSE	73.51	30.62	65.33	37.62	68.56	34.64	69.13	34.29
	± 0.99	± 0.42	± 0.24	± 0.09	± 0.03	± 0.03	# 3	# 2
Co-Boost	73.19	30.56	65.40	37.66	68.55	34.66	69.05	34.29
	± 0.72	± 0.33	± 0.09	± 0.19	± 0.09	± 0.21	# 4	# 2
Ours	79.64	44.86	71.82	47.57	70.31	40.31	73.92	44.25
	± 0.94	± 2.04	± 0.34	± 0.98	± 0.06	± 0.11	# 1	# 1

non-IID data. **(O5)** FedGTA performs worst because its aggregation is based on the unreliable local models’ predictions under non-IID data in a single round. FedSpray focuses on minor classes, but it requires numerous communication for optimization, offering no advantage over others.

To answer **Q2**, we conduct experiments on large-scale graph datasets increasing the number of clients from 10 to 40. The experimental results under the Louvain and Metis partition are reported in Table VI and Table VII, respectively. We make the following 3 observations. **(O1)** Our method consistently outperforms others across different partitions, achieving at least a +0.94% improvement in accuracy and +4.02% in F1-macro. This highlights the superior scalability of our method for large graphs and more clients. **(O2)** FGSSL encounters out-of-memory issues with large-scale graphs due to its high computational and memory requirements. Similarly, FedTAD struggles with the out-of-memory problem when processing graphs with millions of nodes due to its graph diffusion operation. **(O3)** Excluding our method, DENSE performs the best. FedGTA and FedPUB even perform worse than FedAvg with fine-tuning, indicating their lack of robustness with large graph datasets in a single communication round.

In addition to improving accuracy, our method consistently achieves a significant increase in F1-macro, an often overlooked aspect in previous studies. This improvement in F1-macro highlights that our method enhances both personalization and generalization, resulting in more robust models.

2) *Ablation Study*: To answer **Q3**, we conduct the ablation study to evaluate the performance gain of our method. We compare our method with 5 variants: 1) ft: we only fine-tune M_G to obtain M_i on local graph data, 2) ft_imb: we fine-tune

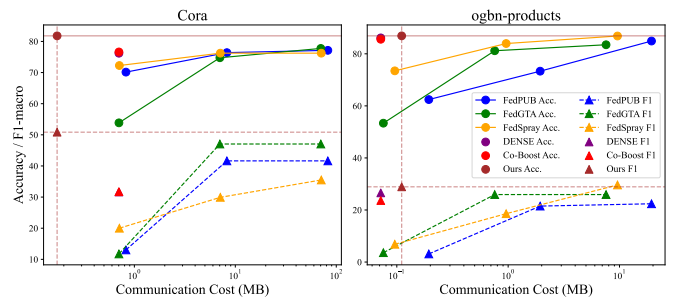


Fig. 9: Communication costs and performance comparison.

with weighted cross entropy loss to handle data imbalance, 3) ft_dist: in the second stage fine-tuning, we perform distillation on all nodes by setting all γ_i to a fixed value in Eq. 18; 4) nd_ft_dist: we perform node adaptive distillation along with fine-tuning, without HRE, 5) ours: we perform the complete method (including HRE and personalized training with node-adaptive distillation), and 6) hre_nd_dist: we perform complete method but without fine-tuning based on M_G from the first stage, instead training a model from scratch with cross-entropy loss and node-adaptive distillation.

Fig. 7 and Fig. 8 show our experimental results of accuracy and F1-macro under Louvain and Metis partition, respectively. We make the following 5 observations. **(O1)** Comparing ft and ft_imb, the weighted cross entropy loss in ft_imb cannot effectively address the non-IID graph data. It improves the F1-macro but at the cost of an accuracy drop. We believe the reasons are that it’s hard to determine the proper weights under extreme non-IID scenarios and class-wise weights are inflexible. **(O2)** Comparing ft and ft_dist, a fixed distillation cannot balance the improvements of accuracy and F1-macro. We believe the reason is that it does not distinguish the majority and minority in the distillation. For nodes in major classes with high homophily, the global knowledge of M_G may have a negative impact, as demonstrated by the left sub-figure in Fig 6. **(O3)** Comparing ft and nd_ft_dist, the node adaptive distillation is more flexible in determining when to introduce the global knowledge of M_G in fine-tuning. Thus nd_ft_dist achieves better accuracy and F1-macro. **(O4)** Comparing nd_ft_dist and ours, the HRE strategy further improves performance by generating a higher-quality global pseudo-graph through more precise estimations. **(O5)** Comparing ours and hre_nd_dist, we conclude that M_G provides better and necessary start-point for fine-tuning. Training the local personalized model from scratch, even with node-adaptive distillation and HRE, leads to a significant performance drop.

We make a further ablation at the client level in Fig. 6, evaluating different methods on a client using the CiteSeer dataset with the Louvain partition. As shown in the middle figure, class 3 and class 5 are regarded as major classes due to their larger quantity and relatively high homophily, while class 2 and class 1 are regarded as minor classes with fewer nodes and lower homophily. We make the following 3 observations. **(O1)** Compared to M_G , the ft method shows performance

TABLE VI: Performance on two large-scale datasets under Louvain partition. OOM represents out-of-memory and FGSSL encounters OOM problems on large-scale datasets.

Louvain	ogbn-arxiv						ogbn-products						Avg. Acc.	Avg. F1
	10 Clients		20 Clients		40 Clients		10 Clients		20 Clients		40 Clients			
	Acc.	F1	Acc.	F1	Acc.	F1	Acc.	F1	Acc.	F1	Acc.	F1		
Standalone	66.46 ±0.24	16.59 ±0.57	66.56 ±0.16	13.53 ±0.34	65.58 ±0.23	12.88 ±0.61	85.25 ±0.02	22.35 ±0.19	86.44 ±0.01	17.34 ±0.05	86.62 ±0.01	14.16 ±0.03	76.15 # 6	16.14 # 6
FedAvg	67.13 ±0.14	18.46 ±0.23	67.17 ±0.12	15.33 ±0.44	66.09 ±0.01	14.06 ±0.09	85.34 ±0.04	22.80 ±0.04	86.48 ±0.01	17.57 ±0.12	86.65 ±0.01	14.48 ±0.08	76.48 # 4	17.12 # 4
FedPUB	65.34 ±0.28	12.50 ±0.20	65.83 ±0.33	10.32 ±0.53	63.07 ±0.26	8.52 ±0.35	83.91 ±0.31	17.29 ±0.52	83.47 ±1.18	11.23 ±0.74	81.51 ±1.07	8.92 ±0.40	73.86 # 7	11.46 # 7
FedGTA	58.30 ±0.30	12.22 ±0.26	57.59 ±1.39	7.72 ±0.67	54.03 ±0.64	6.14 ±0.29	75.87 ±0.04	16.58 ±0.15	79.04 ±0.00	12.15 ±0.10	74.92 ±0.38	8.21 ±0.11	66.63 # 8	10.50 # 8
FedTAD	68.77 ±0.12	27.33 ±0.50	68.90 ±0.14	23.31 ±0.22	67.07 ±0.08	19.41 ±0.06	OOM							
FedSpray	68.68 ±0.05	19.90 ±0.16	68.88 ±0.14	17.56 ±0.27	67.25 ±0.04	15.90 ±0.29	84.06 ±0.11	20.80 ±0.05	85.43 ±0.09	16.08 ±0.10	85.72 ±0.05	13.40 ±0.03	76.67 # 3	17.27 # 3
DENSE	68.80 ±0.04	27.60 ±0.36	68.81 ±0.04	22.97 ±0.18	67.02 ±0.04	19.51 ±0.05	86.12 ±0.03	26.58 ±0.06	86.95 ±0.01	21.14 ±0.00	86.92 ±0.01	17.12 ±0.12	77.44 # 2	22.49 # 2
Co-Boost	66.27 ±0.08	16.37 ±0.14	66.77 ±0.11	13.90 ±0.14	65.76 ±0.12	13.12 ±0.12	85.24 ±0.00	22.31 ±0.11	86.43 ±0.01	17.35 ±0.14	86.62 ±0.01	14.18 ±0.08	76.18 # 5	16.21 # 5
Ours	70.93 ±0.59	36.66 ±0.22	70.61 ±0.05	32.28 ±0.68	68.16 ±0.10	24.99 ±0.69	86.63 ±0.02	27.21 ±0.15	87.03 ±0.00	21.87 ±0.05	86.94 ±0.03	17.62 ±0.16	78.38 # 1	26.77 # 1

TABLE VII: Performance on two large-scale datasets under Metis partition. FGSSL encounters OOM problems.

Metis	ogbn-arxiv						ogbn-products						Avg. Acc.	Avg. F1
	10 Clients		20 Clients		40 Clients		10 Clients		20 Clients		40 Clients			
	Acc.	F1	Acc.	F1	Acc.	F1	Acc.	F1	Acc.	F1	Acc.	F1		
Standalone	66.39 ±0.26	24.05 ±0.70	66.77 ±0.17	19.76 ±0.49	67.06 ±0.21	15.70 ±0.59	85.57 ±0.02	23.54 ±0.10	86.44 ±0.00	18.32 ±0.14	86.92 ±0.01	16.33 ±0.24	76.52 # 5	19.62 # 5
FedAvg	67.04 ±0.13	26.06 ±0.66	67.54 ±0.10	21.68 ±0.16	67.57 ±0.19	17.31 ±0.51	85.63 ±0.01	24.16 ±0.27	86.52 ±0.00	19.04 ±0.09	86.97 ±0.02	16.87 ±0.22	76.88 # 4	20.85 # 3
FedPUB	64.86 ±0.62	18.29 ±1.14	65.41 ±0.34	14.45 ±0.59	65.44 ±0.38	11.86 ±0.66	84.43 ±0.56	17.24 ±0.64	83.94 ±1.18	11.66 ±0.60	83.89 ±0.97	9.50 ±0.26	74.66 # 7	13.83 # 7
FedGTA	55.90 ±1.23	12.72 ±1.53	58.76 ±0.74	10.77 ±0.44	63.32 ±1.18	4.56 ±0.67	74.36 ±0.34	16.67 ±0.19	78.35 ±0.06	13.81 ±0.26	77.97 ±0.20	9.83 ±0.16	68.11 # 8	11.39 # 8
FedTAD	68.96 ±0.28	34.91 ±0.20	69.29 ±0.07	29.84 ±0.34	69.27 ±0.02	24.16 ±0.13	OOM							
FedSpray	68.21 ±0.18	26.57 ±0.17	68.86 ±0.44	22.49 ±0.44	69.04 ±0.13	20.01 ±0.46	86.45 ±0.05	22.02 ±0.06	85.28 ±0.05	17.31 ±0.04	86.01 ±0.03	15.50 ±0.03	77.31 # 3	20.65 # 4
DENSE	68.89 ±0.04	34.34 ±0.34	69.21 ±0.15	29.31 ±0.54	69.33 ±0.03	24.46 ±0.31	86.43 ±0.03	28.42 ±0.25	86.97 ±0.00	22.94 ±0.12	87.03 ±0.01	16.86 ±0.04	77.98 # 2	26.06 # 2
Co-Boost	66.22 ±0.02	23.58 ±0.18	66.72 ±0.06	19.48 ±0.28	67.06 ±0.09	16.06 ±0.19	85.59 ±0.03	23.63 ±0.25	86.43 ±0.01	18.51 ±0.24	86.91 ±0.02	16.34 ±0.17	76.49 # 6	19.60 # 6
Ours	71.06 ±0.09	41.35 ±0.37	70.87 ±0.18	36.06 ±0.43	70.41 ±0.05	30.01 ±0.05	86.90 ±0.01	28.90 ±0.05	87.15 ±0.02	23.41 ±0.26	87.30 ±0.01	20.75 ±0.13	78.95 # 1	30.08 # 1

gain on major class 3 (+1.57%) and class 5 (+0.56%) but degrades performance on minor class 4 (-1.09%), class 2 (-2.78%), and class 1 (-3.22%). The performance differences after fine-tuning, shown in the left figure, align with the H values in the middle figure, highlighting the limitations of fine-tuning. (O2) The ft_dist method cannot handle this limitation effectively. With a fixed γ_i , the performance on major class 5 worsens (-0.42%), and the performance on minor classes still degrades. This phenomenon motivates us to develop node-adaptive distillation. (O3) Our method, with Class-aware Distillation Factor w_{dist} and node adaptive distillation, boosts performance on all classes by more than ($> +2.4%$).

We further justify the rationale for considering homophily in determining the major classes by H values in Eq. 3. The right figure of Fig. 6 shows that class 1 and class 4 have slightly more nodes than class 3, but their average homophily is low (< 0.6), leading to less compact communities in the

local graph. As a result, these classes are often neglected during fine-tuning, causing performance drops of -3.22% and -1.09%, respectively. In contrast, although class 3 has fewer nodes, its high average homophily (> 0.7) results in compact connections, allowing it to dominate the fine-tuning process with a performance improvement of +1.57%.

3) *Performance under Model Heterogeneity:* To answer Q4, we conduct experiments on 10 clients with heterogeneous models. The model configuration is detailed in Sec. V-A0d. Under model heterogeneity, most FGL and pFGL methods (except FedTAD and FedSpray) do not work since they rely on the model parameter aggregation. Thus we compare our method with FedTAD, FedSpray, DENSE, and Co-Boost. The results under Louvain and Metis partitions are presented in Table IV and Table V. The results demonstrate the superior performance of our method in both accuracy and F1-macro.

TABLE VIII: Performance on three inductive datasets under Louvain partition. OOM represents out-of-memory.

Louvain	Flickr				Reddit						Reddit2						Avg. Acc.	Avg. F1
	10 Clients		20 Clients		10 Clients		20 Clients		40 Clients		10 Clients		20 Clients		40 Clients			
	Acc.	F1	Acc.	F1	Acc.	F1	Acc.	F1	Acc.	F1	Acc.	F1	Acc.	F1	Acc.	F1		
Standalone	44.97	12.84	42.10	15.39	90.35	28.79	89.90	13.08	86.32	10.23	91.92	32.53	91.09	16.52	88.17	12.08		
	± 0.70	± 0.06	± 0.14	± 0.25	± 0.02	± 0.07	± 0.06	± 0.21	± 0.03	± 0.10	± 0.01	± 0.20	± 0.02	± 0.04	± 0.06	± 0.24		
FedAvg	45.50	13.66	28.86	13.55	80.75	16.85	83.99	7.81	83.01	6.16	82.86	19.20	85.94	8.48	84.23	6.92		
	± 0.97	± 0.20	± 1.96	± 0.36	± 0.81	± 0.49	± 0.28	± 0.08	± 1.12	± 0.34	± 0.62	± 0.44	± 0.30	± 0.06	± 0.25	± 0.10		
FedPUB	42.17	8.32	42.06	8.31	90.74	27.86	90.34	11.95	87.11	8.54	92.03	30.37	91.23	13.96	89.04	10.16		
	± 0.00	± 0.00	± 0.00	± 0.00	± 0.02	± 0.01	± 0.08	± 0.27	± 0.25	± 0.15	± 0.02	± 0.09	± 0.02	± 0.11	± 0.03	± 0.01		
FGSSL	46.39	14.25	42.86	14.30	OOM													
	± 0.42	± 0.33	± 0.28	± 0.10	OOM													
FedGTA	29.99	14.38	40.78	14.11	90.35	28.76	89.83	12.90	85.35	9.98	91.91	32.71	91.14	16.64	87.52	12.32		
	± 1.71	± 1.15	± 4.26	± 1.51	± 0.02	± 0.24	± 0.05	± 0.32	± 0.02	± 0.10	± 0.38	± 0.11	± 0.05	± 0.12	± 0.05	± 0.09		
FedTAD	45.44	13.85	41.61	15.88	OOM													
	± 0.47	± 0.50	± 0.42	± 0.31	OOM													
FedSpray	43.08	13.08	42.32	14.03	89.07	27.28	89.41	10.71	86.66	8.07	91.28	31.90	90.51	15.29	88.10	9.76		
	± 0.32	± 1.75	± 1.20	± 0.08	± 0.21	± 0.24	± 0.06	± 0.14	± 0.17	± 0.09	± 0.11	± 0.17	± 0.05	± 0.24	± 0.06	± 0.03		
DENSE	44.60	12.47	42.45	11.67	90.32	30.08	89.89	14.27	86.45	10.90	92.00	34.42	91.25	18.14	88.26	13.34		
	± 0.28	± 0.39	± 0.72	± 1.07	± 0.04	± 0.10	± 0.05	± 0.14	± 0.08	± 0.12	± 0.05	± 0.29	± 0.03	± 0.44	± 0.01	± 0.08		
Co-Boost	45.79	13.52	42.07	15.28	90.35	28.62	89.93	13.08	86.21	10.10	91.94	32.68	91.12	16.62	88.16	12.25		
	± 0.54	± 0.52	± 0.07	± 0.45	± 0.03	± 0.05	± 0.03	± 0.19	± 0.10	± 0.12	± 0.02	± 0.04	± 0.03	± 0.15	± 0.07	± 0.10		
Ours	46.83	14.31	44.00	15.60	90.74	30.09	90.38	15.70	87.63	12.96	92.14	35.51	91.34	18.34	88.81	13.74		
	± 0.44	± 0.04	± 0.29	± 0.47	± 0.11	± 0.49	± 0.05	± 0.47	± 0.16	± 0.52	± 0.05	± 0.15	± 0.03	± 0.18	± 0.09	± 0.08		

TABLE IX: Performance on three inductive datasets under Metis partition. OOM represents out-of-memory.

Metis	Flickr				Reddit						Reddit2						Avg. Acc.	Avg. F1
	10 Clients		20 Clients		10 Clients		20 Clients		40 Clients		10 Clients		20 Clients		40 Clients			
	Acc.	F1	Acc.	F1	Acc.	F1	Acc.	F1	Acc.	F1	Acc.	F1	Acc.	F1	Acc.	F1		
Standalone	47.47	12.89	47.10	13.22	88.80	42.34	87.52	28.22	85.00	12.14	90.86	44.78	89.59	25.35	87.91	14.07		
	± 0.12	± 0.47	± 0.20	± 0.37	± 0.09	± 0.40	± 0.03	± 0.10	± 0.08	± 0.29	± 0.04	± 0.35	± 0.01	± 0.08	± 0.04	± 0.25		
FedAvg	34.80	13.45	33.44	12.89	78.83	24.21	80.71	14.64	84.23	7.09	79.30	26.26	82.90	13.91	84.98	7.77		
	± 3.92	± 0.59	± 2.08	± 0.45	± 0.07	± 0.30	± 0.28	± 0.48	± 0.02	± 0.20	± 0.18	± 0.45	± 0.39	± 0.41	± 0.33	± 0.25		
FedPUB	42.65	10.09	42.10	8.30	88.97	41.01	87.36	26.45	85.25	10.44	90.72	41.66	89.89	22.63	88.34	11.50		
	± 0.40	± 2.14	± 0.00	± 0.00	± 0.18	± 0.18	± 0.56	± 0.71	± 0.21	± 0.22	± 0.07	± 0.30	± 0.06	± 0.31	± 0.03	± 0.23		
FGSSL	47.60	13.61	47.19	14.42	OOM													
	± 0.27	± 0.03	± 0.40	± 0.21	OOM													
FedGTA	35.88	13.04	38.75	11.38	88.82	42.02	87.49	27.95	84.42	12.01	90.80	44.59	89.55	25.47	86.72	13.39		
	± 6.10	± 3.66	± 9.16	± 3.46	± 0.11	± 0.21	± 0.01	± 0.22	± 0.03	± 0.30	± 0.07	± 0.27	± 0.03	± 0.29	± 0.03	± 0.21		
FedTAD	47.55	13.07	47.17	13.03	OOM													
	± 0.08	± 0.23	± 0.13	± 0.38	OOM													
FedSpray	43.77	13.37	43.35	14.00	87.71	41.65	86.66	27.60	85.72	9.09	89.99	43.74	88.99	24.23	87.91	11.36		
	± 1.58	± 0.42	± 0.96	± 0.55	± 0.18	± 0.29	± 0.09	± 0.20	± 0.11	± 0.20	± 0.23	± 0.26	± 0.01	± 0.39	± 0.05	± 0.30		
DENSE	45.26	11.56	44.13	11.45	88.72	44.31	87.60	30.49	85.21	14.18	90.01	46.68	89.97	27.72	88.57	13.92		
	± 0.84	± 0.84	± 0.97	± 0.39	± 0.08	± 0.23	± 0.02	± 0.17	± 0.11	± 0.24	± 0.10	± 0.03	± 0.05	± 0.16	± 0.06	± 0.11		
Co-Boost	47.42	12.90	47.08	13.11	88.71	42.08	87.52	28.09	84.94	12.38	90.81	44.56	89.67	25.62	87.93	14.04		
	± 0.10	± 0.61	± 0.22	± 0.66	± 0.07	± 0.27	± 0.06	± 0.12	± 0.04	± 0.30	± 0.06	± 0.20	± 0.07	± 0.22	± 0.04	± 0.24		
Ours	47.89	13.11	47.08	13.37	89.59	45.31	88.28	31.01	86.80	16.54	91.16	48.56	90.25	30.74	88.57	18.43		
	± 0.11	± 0.34	± 0.27	± 0.24	± 0.10	± 0.36	± 0.01	± 0.47	± 0.07	± 0.47	± 0.04	± 0.31	± 0.07	± 0.25	± 0.12	± 0.39		

4) *Inductive Performance*: To answer **Q5**, we conduct experiments on three inductive graph datasets: Flickr, Reddit, and Reddit2. Since Flickr has lower homophily, we use 2-layer SIGN [70] for better graph learning. The results under Louvain and Metis partitions are shown in Table VIII and Table IX. Our method is scalable and generally performs best, achieving at least +0.78% accuracy and +1.37% F1-macro improvement under Louvain partition and at least +0.67% accuracy and +2.09% F1-macro improvement under Metis partition.

5) *Communication Analysis*: To answer **Q6**, we analyze the communication costs both theoretically and empirically. Our method involves uploading the class-wise statistics ($O(Chd)$) and downloading the generated global pseudo-graph ($O(sd + s^2)$), where s represents the number of nodes in global pseudo-graph). Communication costs of both processes are independent of the model size. Fig. 9 reports the experimental communication costs on a small-scale Cora and a large-scale ogbn-products graph datasets under the Metis partition. Note that we report the performance and costs of 1, 10, and 100 communication rounds for FedPUB, FedGTA and FedSpray. The results demonstrate that, in general, our method achieves

superior performance with lower communication costs.

VI. CONCLUSION AND DISCUSSION

In this paper, we propose the first one-shot personalized federated graph learning method that supports model heterogeneity and Secure Aggregation. Specifically, our method first estimates class-wise feature distribution statistics on each client, augmented by our proposed HRE, and then aggregates these statistics on the server to generate the global pseudo-graph. To further enhance personalization and generalization, we propose a novel two-stage personalized model training with node-adaptive distillation, which balances local information and global insights from the global pseudo-graph. Extensive experiments demonstrate our method achieves state-of-the-art performance in terms of both accuracy and F1-macro across various settings, significantly surpassing existing baselines. Our method not only addresses critical limitations in integrating OFL and pFGL but also mitigates biases, improving the generalization, particularly for minorities. Future work will focus on extending our method to handle graphs with diverse properties (e.g., heterophilic and heterogeneous graphs) and more graph-centric tasks.

REFERENCES

- [1] L. He, X. Wang, D. Wang, H. Zou, H. Yin, and G. Xu, "Simplifying graph-based collaborative filtering for recommendation," in *Proceedings of the sixteenth ACM international conference on web search and data mining*, 2023, pp. 60–68.
- [2] Z. Zhou, L. Zhang, and N. Yang, "Contrastive collaborative filtering for cold-start item recommendation," in *Proceedings of the ACM Web Conference 2023*, 2023, pp. 928–937.
- [3] X. Cai, C. Huang, L. Xia, and X. Ren, "Lightgcl: Simple yet effective graph contrastive learning for recommendation," *arXiv preprint arXiv:2302.08191*, 2023.
- [4] S. Yang, Z. Zhang, J. Zhou, Y. Wang, W. Sun, X. Zhong, Y. Fang, Q. Yu, and Y. Qi, "Financial risk analysis for smes with graph-based supply chain mining," in *Proceedings of the Twenty-Ninth International Conference on International Joint Conferences on Artificial Intelligence*, 2021, pp. 4661–4667.
- [5] Y. Qiu, "Default risk assessment of internet financial enterprises based on graph neural network," in *2023 IEEE 6th Information Technology, Networking, Electronic and Automation Control Conference (ITNEC)*, vol. 6. IEEE, 2023, pp. 592–596.
- [6] W. Hyun, J. Lee, and B. Suh, "Anti-money laundering in cryptocurrency via multi-relational graph neural network," in *Pacific-Asia Conference on Knowledge Discovery and Data Mining*. Springer, 2023, pp. 118–130.
- [7] B. Pfeifer, A. Saranti, and A. Holzinger, "Gnn-subnet: disease subnetwork detection with explainable graph neural networks," *Bioinformatics*, vol. 38, no. Supplement_2, pp. ii120–ii126, 2022.
- [8] Z. Qu, T. Yao, X. Liu, and G. Wang, "A graph convolutional network based on univariate neurodegeneration biomarker for alzheimer's disease diagnosis," *IEEE Journal of Translational Engineering in Health and Medicine*, vol. 11, pp. 405–416, 2023.
- [9] D. Bang, S. Lim, S. Lee, and S. Kim, "Biomedical knowledge graph learning for drug repurposing by extending guilt-by-association to multiple layers," *Nature Communications*, vol. 14, no. 1, p. 3570, 2023.
- [10] J. Gasteiger, A. Bojchevski, and S. Günnemann, "Predict then propagate: Graph neural networks meet personalized pagerank," *arXiv preprint arXiv:1810.05997*, 2018.
- [11] A. Iscen, G. Tolias, Y. Avrithis, and O. Chum, "Label propagation for deep semi-supervised learning," in *Proceedings of the IEEE/CVF conference on computer vision and pattern recognition*, 2019, pp. 5070–5079.
- [12] Z. Wu, S. Pan, F. Chen, G. Long, C. Zhang, and S. Y. Philip, "A comprehensive survey on graph neural networks," *IEEE transactions on neural networks and learning systems*, vol. 32, no. 1, pp. 4–24, 2020.
- [13] C. Zhang, D. Song, C. Huang, A. Swami, and N. V. Chawla, "Heterogeneous graph neural network," in *Proceedings of the 25th ACM SIGKDD international conference on knowledge discovery & data mining*, 2019, pp. 793–803.
- [14] P. Voigt and A. Von dem Bussche, "The eu general data protection regulation (gdpr)," *A Practical Guide, 1st Ed., Cham: Springer International Publishing*, vol. 10, no. 3152676, pp. 10–5555, 2017.
- [15] S. Ji, P. Mittal, and R. Beyah, "Graph data anonymization, de-anonymization attacks, and de-anonymizability quantification: A survey," *IEEE Communications Surveys & Tutorials*, vol. 19, no. 2, pp. 1305–1326, 2016.
- [16] Y. Li, M. Purcell, T. Rakotoarivelo, D. Smith, T. Ranbaduge, and K. S. Ng, "Private graph data release: A survey," *ACM Computing Surveys*, vol. 55, no. 11, pp. 1–39, 2023.
- [17] G. Hübscher, V. Geist, D. Auer, A. Ekelhart, R. Mayer, S. Nadschläger, and J. Küng, "Graph-based managing and mining of processes and data in the domain of intellectual property," *Information Systems*, vol. 106, p. 101844, 2022.
- [18] X. Fu, B. Zhang, Y. Dong, C. Chen, and J. Li, "Federated graph machine learning: A survey of concepts, techniques, and applications," *ACM SIGKDD Explorations Newsletter*, vol. 24, no. 2, pp. 32–47, 2022.
- [19] D. Wang, C. Li, S. Wen, S. Nepal, and Y. Xiang, "Man-in-the-middle attacks against machine learning classifiers via malicious generative models," *IEEE Transactions on Dependable and Secure Computing*, vol. 18, no. 5, pp. 2074–2087, 2020.
- [20] H. Yin, A. Mallya, A. Vahdat, J. M. Alvarez, J. Kautz, and P. Molchanov, "See through gradients: Image batch recovery via gradinversion," in *Proceedings of the IEEE/CVF conference on computer vision and pattern recognition*, 2021, pp. 16337–16346.
- [21] V. Mothukuri, R. M. Parizi, S. Pouriyeh, Y. Huang, A. Dehghantanha, and G. Srivastava, "A survey on security and privacy of federated learning," *Future Generation Computer Systems*, vol. 115, pp. 619–640, 2021.
- [22] G. Zhu, D. Li, H. Gu, Y. Han, Y. Yao, L. Fan, and Q. Yang, "Evaluating membership inference attacks and defenses in federated learning," *arXiv preprint arXiv:2402.06289*, 2024.
- [23] T. Li, A. K. Sahu, A. Talwalkar, and V. Smith, "Federated learning: Challenges, methods, and future directions," *IEEE signal processing magazine*, vol. 37, no. 3, pp. 50–60, 2020.
- [24] P. Kairouz, H. B. McMahan, B. Avent, A. Bellet, M. Bennis, A. N. Bhagoji, K. Bonawitz, Z. Charles, G. Cormode, R. Cummings *et al.*, "Advances and open problems in federated learning," *Foundations and trends® in machine learning*, vol. 14, no. 1–2, pp. 1–210, 2021.
- [25] R. Dai, L. Shen, F. He, X. Tian, and D. Tao, "Displf: Towards communication-efficient personalized federated learning via decentralized sparse training," in *International conference on machine learning*. PMLR, 2022, pp. 4587–4604.
- [26] N. Guha, A. Talwalkar, and V. Smith, "One-shot federated learning," *arXiv preprint arXiv:1902.11175*, 2019.
- [27] J. Zhang, C. Chen, B. Li, L. Lyu, S. Wu, S. Ding, C. Shen, and C. Wu, "Dense: Data-free one-shot federated learning," *Advances in Neural Information Processing Systems*, vol. 35, pp. 21414–21428, 2022.
- [28] J. Baek, W. Jeong, J. Jin, J. Yoon, and S. J. Hwang, "Personalized subgraph federated learning," in *International conference on machine learning*. PMLR, 2023, pp. 1396–1415.
- [29] X. Li, Z. Wu, W. Zhang, Y. Zhu, R.-H. Li, and G. Wang, "Fedgta: Topology-aware averaging for federated graph learning," *arXiv preprint arXiv:2401.11755*, 2024.
- [30] Y. Zhu, X. Li, Z. Wu, D. Wu, M. Hu, and R.-H. Li, "Fedtd: Topology-aware data-free knowledge distillation for subgraph federated learning," *arXiv preprint arXiv:2404.14061*, 2024.
- [31] R. Dai, Y. Zhang, A. Li, T. Liu, X. Yang, and B. Han, "Enhancing one-shot federated learning through data and ensemble co-boosting," *arXiv preprint arXiv:2402.15070*, 2024.
- [32] H. Zeng, M. Xu, T. Zhou, X. Wu, J. Kang, Z. Cai, and D. Niyato, "One-shot-but-not-degraded federated learning," in *Proceedings of the 32nd ACM International Conference on Multimedia*, 2024, pp. 11070–11079.
- [33] C. E. Heinbaugh, E. Luz-Ricca, and H. Shao, "Data-free one-shot federated learning under very high statistical heterogeneity," in *The Eleventh International Conference on Learning Representations*, 2023.
- [34] M. Yang, S. Su, B. Li, and X. Xue, "Feddeo: Description-enhanced one-shot federated learning with diffusion models," *arXiv preprint arXiv:2407.19953*, 2024.
- [35] —, "Exploring one-shot semi-supervised federated learning with pre-trained diffusion models," in *Proceedings of the AAAI Conference on Artificial Intelligence*, vol. 38, no. 15, 2024, pp. 16325–16333.
- [36] R. Rombach, A. Blattmann, D. Lorenz, P. Esser, and B. Ommer, "High-resolution image synthesis with latent diffusion models," in *Proceedings of the IEEE/CVF conference on computer vision and pattern recognition*, 2022, pp. 10684–10695.
- [37] K. Bonawitz, V. Ivanov, B. Kreuter, A. Marcedone, H. B. McMahan, S. Patel, D. Ramage, A. Segal, and K. Seth, "Practical secure aggregation for privacy-preserving machine learning," in *proceedings of the 2017 ACM SIGSAC Conference on Computer and Communications Security*, 2017, pp. 1175–1191.
- [38] J. So, C. He, C.-S. Yang, S. Li, Q. Yu, R. E. Ali, B. Guler, and S. Avestimehr, "Lightsecagg: a lightweight and versatile design for secure aggregation in federated learning," *Proceedings of Machine Learning and Systems*, vol. 4, pp. 694–720, 2022.
- [39] T. N. Kipf and M. Welling, "Semi-supervised classification with graph convolutional networks," *arXiv preprint arXiv:1609.02907*, 2016.
- [40] C. Wu, F. Wu, Y. Cao, Y. Huang, and X. Xie, "Fedgnn: Federated graph neural network for privacy-preserving recommendation," *arXiv preprint arXiv:2102.04925*, 2021.
- [41] C. Zhang, G. Long, T. Zhou, Z. Zhang, P. Yan, and B. Yang, "Gpfedrec: Graph-guided personalization for federated recommendation," in *Proceedings of the 30th ACM SIGKDD Conference on Knowledge Discovery and Data Mining*, 2024, pp. 4131–4142.
- [42] B. Yan, Y. Cao, H. Wang, W. Yang, J. Du, and C. Shi, "Federated heterogeneous graph neural network for privacy-preserving recommendation," in *Proceedings of the ACM on Web Conference 2024*, 2024, pp. 3919–3929.

- [43] T. Tang, Z. Han, Z. Cai, S. Yu, X. Zhou, T. Oseni, and S. K. Das, "Personalized federated graph learning on non-iid electronic health records," *IEEE Transactions on Neural Networks and Learning Systems*, 2024.
- [44] M. Chen, W. Zhang, Z. Yuan, Y. Jia, and H. Chen, "Fede: Embedding knowledge graphs in federated setting," in *Proceedings of the 10th International Joint Conference on Knowledge Graphs*, 2021, pp. 80–88.
- [45] H. Xie, J. Ma, L. Xiong, and C. Yang, "Federated graph classification over non-iid graphs," *Advances in neural information processing systems*, vol. 34, pp. 18 839–18 852, 2021.
- [46] Y. Tan, Y. Liu, G. Long, J. Jiang, Q. Lu, and C. Zhang, "Federated learning on non-iid graphs via structural knowledge sharing," in *Proceedings of the AAAI conference on artificial intelligence*, vol. 37, no. 8, 2023, pp. 9953–9961.
- [47] B. Wang, A. Li, M. Pang, H. Li, and Y. Chen, "Graphfl: A federated learning framework for semi-supervised node classification on graphs," in *2022 IEEE International Conference on Data Mining (ICDM)*. IEEE, 2022, pp. 498–507.
- [48] C. Chen, Z. Xu, W. Hu, Z. Zheng, and J. Zhang, "Fedgl: Federated graph learning framework with global self-supervision," *Information Sciences*, vol. 657, p. 119976, 2024.
- [49] W. Huang, G. Wan, M. Ye, and B. Du, "Federated graph semantic and structural learning," *arXiv preprint arXiv:2406.18937*, 2024.
- [50] X. Li, Z. Wu, W. Zhang, H. Sun, R.-H. Li, and G. Wang, "Adafgl: A new paradigm for federated node classification with topology heterogeneity," *arXiv preprint arXiv:2401.11750*, 2024.
- [51] K. Zhang, C. Yang, X. Li, L. Sun, and S. M. Yiu, "Subgraph federated learning with missing neighbor generation," *Advances in Neural Information Processing Systems*, vol. 34, pp. 6671–6682, 2021.
- [52] K. Zhang, L. Sun, B. Ding, S. M. Yiu, and C. Yang, "Deep efficient private neighbor generation for subgraph federated learning," in *Proceedings of the 2024 SIAM International Conference on Data Mining (SDM)*. SIAM, 2024, pp. 806–814.
- [53] Y. Yao, W. Jin, S. Ravi, and C. Joe-Wong, "Fedgcn: Convergence-communication tradeoffs in federated training of graph convolutional networks," *Advances in neural information processing systems*, vol. 36, 2024.
- [54] X. Fu, Z. Chen, B. Zhang, C. Chen, and J. Li, "Federated graph learning with structure proxy alignment," in *Proceedings of the 30th ACM SIGKDD Conference on Knowledge Discovery and Data Mining*, 2024, pp. 827–838.
- [55] H. Yin, P. Molchanov, J. M. Alvarez, Z. Li, A. Mallya, D. Hoiem, N. K. Jha, and J. Kautz, "Dreaming to distill: Data-free knowledge transfer via deepinversion," in *Proceedings of the IEEE/CVF conference on computer vision and pattern recognition*, 2020, pp. 8715–8724.
- [56] Y. Diao, Q. Li, and B. He, "Towards addressing label skews in one-shot federated learning," in *The Eleventh International Conference on Learning Representations*, 2023.
- [57] Y. Zhou, G. Pu, X. Ma, X. Li, and D. Wu, "Distilled one-shot federated learning," *arXiv preprint arXiv:2009.07999*, 2020.
- [58] R. Song, D. Liu, D. Z. Chen, A. Festag, C. Trinitis, M. Schulz, and A. Knoll, "Federated learning via decentralized dataset distillation in resource-constrained edge environments," in *2023 International Joint Conference on Neural Networks (IJCNN)*. IEEE, 2023, pp. 1–10.
- [59] W. Jin, L. Zhao, S. Zhang, Y. Liu, J. Tang, and N. Shah, "Graph condensation for graph neural networks," *arXiv preprint arXiv:2110.07580*, 2021.
- [60] M. Liu, S. Li, X. Chen, and L. Song, "Graph condensation via receptive field distribution matching," *arXiv preprint arXiv:2206.13697*, 2022.
- [61] B. Yang, K. Wang, Q. Sun, C. Ji, X. Fu, H. Tang, Y. You, and J. Li, "Does graph distillation see like vision dataset counterpart?" *Advances in Neural Information Processing Systems*, vol. 36, 2024.
- [62] Z. Xiao, Y. Wang, S. Liu, H. Wang, M. Song, and T. Zheng, "Simple graph condensation," in *Joint European Conference on Machine Learning and Knowledge Discovery in Databases*. Springer, 2024, pp. 53–71.
- [63] Z. Yang, W. Cohen, and R. Salakhudinov, "Revisiting semi-supervised learning with graph embeddings," in *International conference on machine learning*. PMLR, 2016, pp. 40–48.
- [64] W. Hu, M. Fey, M. Zitnik, Y. Dong, H. Ren, B. Liu, M. Catasta, and J. Leskovec, "Open graph benchmark: Datasets for machine learning on graphs," *Advances in neural information processing systems*, vol. 33, pp. 22 118–22 133, 2020.
- [65] H. Zeng, H. Zhou, A. Srivastava, R. Kannan, and V. Prasanna, "Graphsaint: Graph sampling based inductive learning method," *arXiv preprint arXiv:1907.04931*, 2019.
- [66] W. Hamilton, Z. Ying, and J. Leskovec, "Inductive representation learning on large graphs," *Advances in neural information processing systems*, vol. 30, 2017.
- [67] X. Li, Y. Zhu, B. Pang, G. Yan, Y. Yan, Z. Li, Z. Wu, W. Zhang, R.-H. Li, and G. Wang, "Openfgl: A comprehensive benchmarks for federated graph learning," *arXiv preprint arXiv:2408.16288*, 2024.
- [68] H. Zhu and P. Koniusz, "Simple spectral graph convolution," in *International conference on learning representations*, 2021.
- [69] F. Wu, A. Souza, T. Zhang, C. Fifty, T. Yu, and K. Weinberger, "Simplifying graph convolutional networks," in *International conference on machine learning*. PMLR, 2019, pp. 6861–6871.
- [70] F. Frasca, E. Rossi, D. Eynard, B. Chamberlain, M. Bronstein, and F. Monti, "Sign: Scalable inception graph neural networks," *arXiv preprint arXiv:2004.11198*, 2020.